THE JOURNAL OF BIOLOGICAL CHEMISTRY VOL. 285, NO. 13, pp. 10098–10109, March 26, 2010

CB_1 Cannabinoid Receptors Increase Neuronal Precursor Proliferation through AKT/Glycogen Synthase Kinase-3β/β-Catenin Signaling

Received for publication, July 12, 2009, and in revised form, January 15, 2010 Published, JBC Papers in Press, January 18, 2010, DOI 10.1074/jbc.M109.043711

Stefania Trazzi[‡1], Martin Steger[‡1], Valentina Maria Mitrugno[‡], Renata Bartesaghi[‡], and Elisabetta Ciani[‡§2]

From the [‡]Department of Human and General Physiology, University of Bologna, Piazza di Porta San Donato 2, 40126 Bologna and the [§]Center for Applied Biomedical Research, S. Orsola-Malpighi University Hospital, 40138 Bologna, Italy

The endocannabinoid system is involved in the regulation of many physiological effects in the central and peripheral nervous system. Recent findings have demonstrated the presence of a functional endocannabinoid system within neuronal progenitors located in the hippocampus and ventricular/subventricular zone that participates in the regulation of cell proliferation. It is presently unknown whether the endocannabinoid system exerts a widespread effect on neuronal precursors from different neurogenic regions, and very little is known about the signaling by which it regulates neuronal precursor proliferation. Herein, we demonstrate the presence of cannabinoid CB_1 receptors in granule cell precursors (GCPs) during early cerebellar development. Activation of CB_1 receptors by HU-210 promoted GCP proliferation *in vitro*, an effect that was prevented by a selective CB_1 antagonist. Accordingly, *in vivo* experiments showed that GCP proliferation was increased by chronic HU-210 treatment and that in CB_1-deficient mice cell proliferation was significantly lower than in wild-type littermates, indicating that the endocannabinoid system is physiologically involved in regulation of GCP proliferation. The pro-proliferative effect of cannabinoids in GCPs was mediated through the CB_1/AKT/glycogen synthase kinase-3β/β-catenin pathway. Involvement of this pathway was also observed in cultures of neuronal precursors from the subventricular zone, suggesting that this pathway may be a general mechanism by which endocannabinoids regulate proliferation of neuronal precursors. These observations suggest that endocannabinoids constitute a new family of lipid signaling cues that may exert a widespread effect on neuronal precursor proliferation during brain development.

Cannabinoid drugs such as Δ^9-tetrahydrocannabinol, the principal psychoactive constituent of marijuana, act via signaling pathways consisting of endogenous cannabinoids (endocannabinoids) and their receptors. Among endocannabinoids, the best characterized are arachidonylethanolamide or anandamide and 2-arachidonylglycerol, although additional candidates have been proposed. Two G-protein-coupled cannabinoid receptors, designated CB_1 and CB_2, have been cloned (1, 2). The CB_1 receptor is highly expressed in the central nervous system and is also present in peripheral and extraneuronal sites (3, 4). In contrast, the CB_2 receptor is almost restricted to the immune system (2).

Endocannabinoid signaling pathways have been implicated in a broad range of neurobiological processes, including movement control, cognition, learning and memory, pain relief, and in promoting neuronal survival after cerebral ischemia or trauma (5–9). In addition, pharmacological and gene knock-out studies point to a role for endocannabinoid signaling in promoting brain development (10). For example, the expression of endocannabinoids and cannabinoid receptors appears early in the developing brain (10–13), and the perinatal exposure to synthetic or plant-derived cannabinoids was shown to modify the maturation of neurotransmitter systems and their related behaviors (14). Recent studies have demonstrated the presence of a functional endocannabinoid system in neuronal progenitor cells of the ventricular (VZ)[3] and subventricular zone (SVZ) and subgranular zone of the hippocampal dentate gyrus, where it increases cell proliferation (15–20). Consistent with the proliferation-promoting function of CB_1 receptors, impaired proliferation is observed during cortical development in the VZ/SVZ of CB_1 knock-out mice (16). Conversely, inhibition of the activity of the fatty acid amide hydrolase, an enzyme involved in the breakdown of endocannabinoids (18), elicits an increase in cell proliferation.

The brain regions that have the highest densities of CB_1 receptors are the hippocampal formation, basal ganglia, and cerebellum (21). The majority, if not all, of the cannabinoid receptors in the cerebellum are located on axon terminals of cerebellar granule cells (22), glutamatergic neurons that project to cerebellar Purkinje cells. In rodents, cerebellar granule cells are generated during the first two postnatal weeks from progenitor cells in the outermost layer of the cerebellar cortex, the external granule layer (EGL). The regulation of cerebellar granule precursor proliferation, differentiation, and survival is controlled by a number of extracellular signaling cues (23). Whereas the function of the endocannabinoid system has been extensively studied in differentiated cerebellar granule cells

[1] Both authors equally contributed to this work.

[2] To whom correspondence should be addressed: Dept. of Human and General Physiology, University of Bologna, Piazza di Porta San Donato 2, 40126 Bologna, Italy. Tel.: 39-051-209-1721; Fax: 39-051-251737; E-mail: elisabetta.ciani@unibo.it.

[3] The abbreviations used are: VZ, ventricular; SVZ, subventricular zone; EGL, external granule layer; oEGL, outer EGL; iEGL, inner EGL; GCP, granule cell precursor; ERK, extracellular signal-regulated kinase; PI3K, phosphatidylinositol 3-kinase; P, postnatal day; RT-qPCR, reverse transcriptase quantitative PCR; BrdUrd, 5-bromo-2-deoxyuridine; EGF, epidermal growth factor; LI, labeling index; ANOVA, analysis of variance; DIV, days *in vitro*; GSK-3β, glycogen synthase kinase-3β; AS, antisense oligonucleotides; S, sense oligonucleotides.

(24–27), its potential role in the regulation of cerebellar granule precursor (GCP) proliferation/survival has not been addressed so far.

The activation of the CB_1 receptor is coupled with the inhibition of adenylyl cyclase, the inhibition of voltage-dependent Ca^{2+} channels, and the activation of G-protein-regulated inwardly rectifying K^+ channels (4, 28). In addition, several signaling pathways have been shown to be regulated by the cannabinoid receptors. For instance, the CB_1 receptor has been shown to regulate different members of the mitogen-activated protein kinase family, such as extracellular signal-regulated kinase (ERK) (29, 30), c-Jun N-terminal kinase (31, 32), and p38 (32, 33). The CB_1 receptor can also activate the phosphatidylinositol 3-kinase/protein kinase B (PI3K/AKT) signaling pathway (34, 35). Although the mechanisms by which the endocannabinoid system exerts most of its effects have been elucidated (4), very little is known about the signaling mechanism underlying cannabinoid-regulated neuronal precursor cell proliferation.

In the present work, we examined the presence of cannabinoid receptors in GCP during early cerebellar development; we investigated the role of the cannabinoids in the regulation of GCP proliferation and identified the pathway downstream from the CB_1 receptor implicated in the regulation of neuronal precursor proliferation.

EXPERIMENTAL PROCEDURES

Animals and Treatments—Experimental animals were C57BL/6J mice, wild-type ($CB_1^{+/+}$) and homozygous CB_1 knock-out mice ($CB_1^{-/-}$) (36). Experiments were performed in accordance with the Italian and European Community law for the use of experimental animals and were authorized by the bioethical committee of the University of Bologna. Pregnant mothers were isolated in single cages when pregnancy became evident. C57BL/6J, $CB_1^{+/+}$, and $CB_1^{-/-}$ pups received two subcutaneous injections (injection volume 20 ml/kg) either of HU-210 (100 μg/kg, diluted in phosphate-buffered saline) or phosphate-buffered saline for 3 days, starting at postnatal day 4 (P4). Six hours after the last administration of either HU-210 or phosphate-buffered saline, mice received a single subcutaneous injection (150 μg/g body weight) of BrdUrd (5-bromo-2-deoxyuridine, Sigma) and were sacrificed after 2 h. Pups were killed by decapitation, and the cerebellum was rapidly dissected and fixed by immersion in Glyo-Fixx (Thermo Electron Corp., Waltham, MA) for 24 h.

Cell Cultures and Treatments—Primary cultures of GCPs were prepared from the cerebella of 7-day-old C57BL/6J, $CB_1^{+/+}$, and $CB_1^{-/-}$ mice as previously described (37). Dissociated cells were plated on poly-D-lysine (20 μM, Sigma)-coated dishes at a density of 2×10^3 cells/mm^2 and maintained in Neurobasal A medium (Invitrogen) supplemented with 2% B27 (Invitrogen), 2 mM glutamine, and 100 μg/ml penicillin/50 μg/ml streptomycin (Sigma). Cells were isolated from the rostral telencephalon of newborn (P1–P2) C57BL/6J mice, and neurosphere cultures were obtained as previously reported (38, 39). To obtain neurospheres, cells were cultured in suspension in Dulbecco's modified Eagle's medium/F-12 (1:1) containing B27 supplements (2%), fibroblast growth factor-2 (FGF2, 20 ng/ml), epidermal growth factor (EGF, 20 ng/ml), heparin (5 μg/ml), penicillin (100 units/ml), and antibiotics. Primary neurospheres were dissociated at days 8–10 using Accutase (PAA, Pasching, Austria) to derive secondary neurospheres. The sub-culturing protocol consisted of neurosphere passages carried out every 3–4 days with whole culture media change (with freshly added fibroblast growth factor-2 and EGF). All experiments were done using neurospheres obtained after 3–5 passages from the initially prepared cultures. Cell cultures were kept in a 5% CO_2 humidified atmosphere at 37 °C. Unless specified otherwise, treatments were performed 2 h after cell plating with the following drugs: 0.5 μM (6α*R*,10α*R*)-9-(hydroxymethyl)-6,6-dimethyl-3-(2-methyloctan-2-yl)-6α,7,10,10α-tetrahydrobenzo-[*c*]chromen-1-ol (HU-210 Tocris), 0.1, 0.5, 1, 2, and 5 μM 3-(1,1-dimethylbutyl)-1-deoxy-Δ^8-tetrahydrocannabinol (JWH-133, Tocris), 12.5 μM BML-257 (Cayman), 60 nM Akti-1/2 (Calbiochem), 10 μM LY294002 (Cell Signaling Technology), 0.5 μM wortmannin (Calbiochem), PD158780 (Calbiochem), and 2 μM SR 141716A (*N*-(piperidin-1-yl)-5-(4-chlorophenyl)-1-(2,4-dichlorophenyl)-4-methylpyrazole-3-carboxamide, hydrochloride, contract N01-MH-32005 WA 08928.019, NIMH no. S-705, Chemical Synthesis and Drug Supply Program, NIMH, Research Triangle Institute) for the indicated times.

Immunocytochemistry and Determination of the Labeling Index in Cell Cultures—For immunofluorescence studies, the following primary antibodies were used: anti-neural cell adhesion molecule (N-CAM, 1:200, Sigma), anti-Ki67 (GeneTex, 1:100), anti-β-catenin (1:100, BD Transduction Laboratories), anti-BrdUrd (1:200, Roche Applied Science), anti-CB_1 (L-15-CB_1, 1:200, kindly provided by Dr. Ken Mackie), and β-tubulin III (TubJ, 1:500, Sigma). GCPs, plated on poly-D-lysine-coated coverslips, were cultured for 18 h, then treated with 10 μM BrdUrd for an additional 6 h, fixed, and processed for BrdUrd and β-tubulin III (TubJ, an early neuronal marker) double-fluorescence immunocytochemistry and counterstained with Hoechst 33342, as previously described (40). Fluorescence images, taken from random microscopic fields (10–12 for each coverslip), were superimposed and used to determine the labeling index (LI), defined as percentage of cells co-labeled with BrdUrd and β-tubulin III over total cell number in three independent experiments in duplicate. Pyknotic cells were separately counted to determine the pyknotic LI defined as percentage of pyknotic cells over total cell number. Fluorescence images were taken on an Eclipse TE 2000-S microscope (Nikon, Tokyo, Japan) equipped with a digital camera Sight DS-2MBW (Nikon).

Antisense Experiment—To silence the expression of β-catenin, experiments were performed by using an antisense oligonucleotide (5′-ggAGTTTAACCACAACAGGCAGTcc-3′) and, as a control, a sense oligonucleotide (5′-ggACTGCCTGTTGTG-GTTAAACTcc-3′) (41). Both oligonucleotides (Sigma-Aldrich) were phosphorothioated to make them more resistant to RNase attack. Cultures of GCPs were exposed 2 h after plating to different concentrations of the oligonucleotides for 24 h.

Immunocytochemistry and Determination of β-Catenin Nuclear Localization in Neurosphere Cultures—Neurospheres were harvested on microscope slides by cytospin centrifugation ($212 \times g$, 5 min, Shandon, Thermo, Dreieich, Germany). Specimens were fixed in 4% paraformaldehyde for 20 min. Blocking

was done in 5% goat serum for 30 min followed by incubation with anti-β-catenin (1:100, BD Transduction Laboratories) antibody. Detection was done with Cy3-conjugated anti-mouse antibody (1:200, Jackson ImmunoResearch Laboratories). Nuclear staining was obtained using Hoechst 33342 as previously described (40). Neurospheres were examined at 20× magnification using an Eclipse TE 2000-S microscope (Nikon). Immunofluorescence analysis was performed in a blinded fashion by numerically coding each slide. Digital images were captured using NIS-Elements AR software (Nikon). Only cells with both cellular and nuclear integrity were analyzed. Cellular and nuclear integrity was assessed morphologically. Intact nuclei were defined as well circumscribed oval bodies as delineated by Hoechst staining. To assess β-catenin nuclear translocation, Hoechst and β-catenin images of the same cell were processed using NIS-Elements AR software (Nikon). The perimeter of the nucleus was traced using the Hoechst (blue) counterstaining as a guide to define the nuclear area of each cell, and the intensity of Cy3 staining corresponding to the β-catenin signal was quantified by determining the number of positive (bright) nuclear pixels. Approximately 150 cells were analyzed from each slide (2 slides for each condition; 3 experiments).

Immunohistochemistry and Cell Count—Cerebella from C57BL/6J, $CB_1^{+/+}$, and $CB_1^{-/-}$ mouse pups were embedded in paraffin and cut with a microtome in 8-μm-thick sections. One of eight sections was processed for BrdUrd or anti-cleaved caspase-3 (1:100, Cell Signaling Technology) immunohistochemistry as previously described (42, 43). Cell count was done in the external granular layer (Fig. 6*D*) for BrdUrd-positive cells and in both the external granular layer and internal granule layer for cleaved caspase-3-positive cells, in three lobuli (II, III, and VI) of each sampled section. Cell number was expressed as cells/mm^2.

Laser Capture Microdissection—Frozen 12-μm-thick sections from the cerebellum of P6 C57BL/6J mice were cut with a cryostat, fixed in 70% ethanol, stained briefly with cresyl violet, and dehydrated with xylene. The oEGL of the cerebellum was microdissected from two- three sections using a laser-capture microscope (Eclipse TE 2000-U, Nikon) with the following parameters: spot size, 30 μm; power, 85 milliwatts; and duration, 750–1200 μs.

Real-time RT-qPCR—Total RNA was extracted from cultures of GCPs with Tri Reagent (Sigma) and from laser-captured cerebellar tissue using the Picopure Isolation kit (Arcturus) according to the manufacturer's instructions. cDNA synthesis was achieved with 0.5–1.0 μg of total RNA using the iScript™ cDNA synthesis kit (Bio-Rad) according to the manufacturer's instructions. The efficiency of the used primers was evaluated by calculating the linear regression of Ct data points obtained with a series of different cDNA dilutions and inferring the efficiency from the slope of the line. We used the primers that gave efficiency close to 100%. The used primer sequences were the following: (i) CB_1 (NM_007726), forward (5′-CTGCTGTTGCTGTTCATTGTG-3′) and reverse (5′-CTTGCCATCTTCTGAGGTGTG-3′); (ii) CB_2 (NM_009924), forward (5′-GCCCGAGTCAGAAGTCCGTTC-3′) and reverse (5′-GCCACCTTCCAGCCAACCAGC-3′); (iii) N-MYC (NM_008709), forward (5′-GGTGGCTGCTCCTGCTCGTC-3′) and reverse (5′-TCCTCTTCATCTTCCTCCTCGT-3′); (iv) $GABA_A$ (NM_008072), forward (5′-TGCCGCTCCTGCTGCTCTG-3′) and reverse (5′-GCATAGCCCTCCATTAAGCCATCC-3′); (v) TRPV1 (NM_001001445.1), forward (5′-TGGGAAGGGTGACTCAGAAGAGG-3′) and reverse (5′-TCCTGCGATCATAGAGCCTTGGG-3′); (vi) Cyclin D1 (NM_007631) forward (5′-ACCGCACAACGCACTTTCTTTCC-3′) and reverse (5′-GACCAGCCTCTTCCTCCACTTCC-3′); and (vii) β-actin (NM_007393) forward (5′-AAGTGGTTACAGGAAGTCC-3′) and reverse (5′-ATAATTTACACAGAAGCAATGC-3′). Real-time PCR was performed using a SYBR Premix Ex Taq kit (Takara, Shiga, Japan) according to the manufacturer's instructions in an iQ5 real-time PCR detection system (Bio-Rad). Fluorescence was determined at the last step of every cycle. Real-time PCR assay was done under the following universal conditions: 2 min at 50 °C, 10 min at 95 °C, 50 cycles of denaturation at 95 °C for 15 s, and annealing/extension at 60 °C for 1 min. Relative quantification was performed using the $\Delta\Delta C_t$ method.

Western Blotting—The following antibodies were used: anti-phosphorylated Erk1/2, anti-phospho-AKT-Ser^{473} (1:1000), AKT-Thr^{308} (1:1000), anti-AKT (1:1000), and anti-phospho-GSK-3β-Ser^{9} (1:1000) (Cell Signaling Technology); anti-β-catenin (1:1000, BD Transduction Laboratories); and anti-β-actin (1:2000, Sigma). For the preparation of total cell extracts, cells were lysed in lysis buffer (Tris-HCl, 10 mM, SDS, 2%, dithiothreitol, 10 mM, protease and phosphatase inhibitors cocktails, 1% (Sigma)). For the preparation of nuclear extracts cells were allowed to swell and lysed in hypotonic buffer (Hepes, 10 mM, NaCl, 50 mM, EDTA, 1 mM, Nonidet P-40, 0.1%, dithiothreitol, 1 mM, phenylmethylsulfonyl fluoride, 1 mM, pH 8) for 10 min at 4 °C. After centrifugation, nuclei were extracted with hypertonic salt buffer (Hepes, 20 mM, NaCl, 420 mM, EDTA, 1 mM, dithiothreitol, 1 mM, glycerol, 10%, phenylmethylsulfonyl fluoride, 1 mM, pH 8). Cells extracts were immediately processed by Western blot or kept frozen (−80 °C) until assayed. Sample protein concentration was estimated by the Lowry method (44). Equivalent amounts (40 μg) of protein were subjected to electrophoresis on a 10% SDS-polyacrylamide gel. Densitometric analysis of digitized images was performed with Scion Image software (Scion Corp., Frederick, MD), and the intensity for each band was normalized to the intensity of the corresponding β-actin band.

Statistics—Data are expressed as mean ± S.E., and statistical significance was assessed by two-way analysis of variance (ANOVA), followed by Bonferroni post hoc test or by the two-tailed *t* test. Significance was set to $p \leq 0.05$. Statistical analysis was performed using GraphPad Prism 4.0.

RESULTS

Expression of CB_1 and CB_2 Receptors in Cerebellar Granule Cell Precursors in Culture—Recent evidence suggests that endocannabinoid signaling plays a role in neurogenesis in the subventricular zone and subgranular layer of the hippocampal dentate gyrus (see the introduction). However, it is presently unknown whether cannabinoids are able to promote proliferation of cerebellar GCPs. To determine whether GCPs express cannabinoid receptors, we examined CB_1 protein and gene

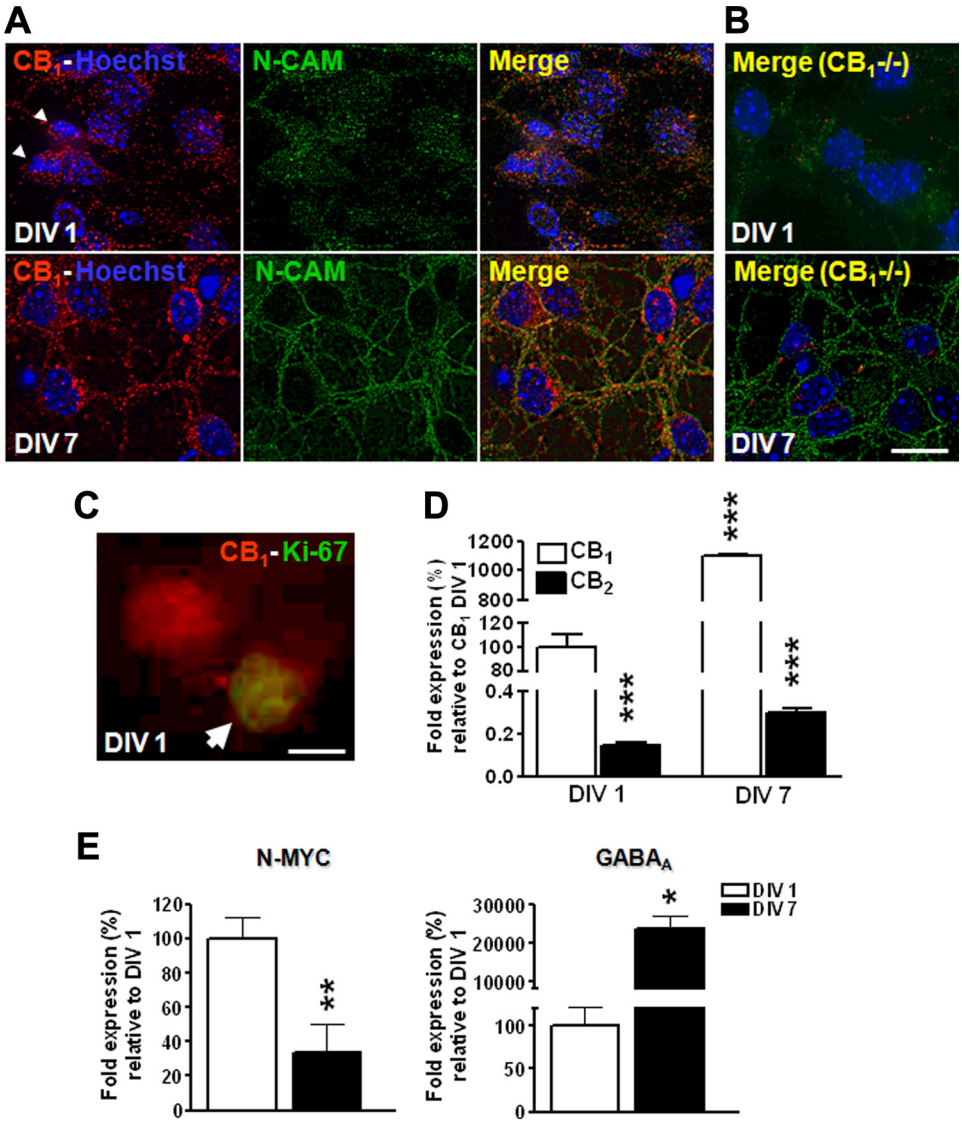

FIGURE 1. **Expression of CB_1 and CB_2 receptors in GCPs.** *A* and *B*, double immunofluorescence staining for CB_1 (*red*) and N-CAM (*green*) of cerebellar granule cells derived from C57BL/6J (*A*) and $CB_1^{-/-}$ (*B*) P7 mice cultured for 1 day (*DIV 1*) or 7 days (*DIV 7*) *in vitro*. Hoechst staining of nuclei was used to reveal the total number of cells in culture (*blue*). The *arrows* indicate condensed mitotic chromosomes of a cell immunostained for CB_1 receptors. *Scale bar* in *B*: 10 μm applies to *A* and *B*. *C*, double immunofluorescence staining for CB_1 (*red*) and Ki-67 (*green*) of cerebellar granule cells derived from P7 mice and cultured for 1 day (*DIV 1*) *in vitro*. *Scale bar*: 5 μm. *D*, CB_1 and CB_2 mRNA expression, quantified by RT-qPCR, in culture of cerebellar granule cells at DIV 1 and DIV 7. *E*, N-Myc and $GABA_A$ receptor expression, quantified by RT-qPCR, in cultures of cerebellar granule cells at DIV 1 and DIV 7. Data in *C* and *D* are expressed as mean ± S.E. of three independent experiments. *, $p < 0.05$; **, $p < 0.01$; ***, $p < 0.001$ (Bonferroni's test after ANOVA).

expression in cultures of GCPs from mouse pups using CB_1 antibody immunocytochemistry and quantitative real-time PCR (RT-qPCR). About 98% of total cells were faintly but clearly double labeled with antibodies for CB_1 and N-CAM (a neuronal marker) 24 h after cell plating (DIV 1) (Fig. 1*A*), indicating that CB_1 receptors were expressed by neuronal precursors. On the other hand, CB_1 immunoreactivity was not localized in glial fibrillary acidic protein-positive cells (data not shown), indicating that CB_1-positive cells were not astrocytes. Actively dividing cells, recognizable by the condensed chromosomes typical of the late M phase of the cell cycle (*white arrows* in Fig. 1*A*), were immunoreactive for the CB_1 receptor, indicating that dividing GCPs were, at this stage, already expressing CB_1 receptors. Because the expression of the Ki-67 protein is strictly associated with cell proliferation, double immunostaining for CB_1 and Ki-67 observed in GCP cultures at DIV 1 further confirmed the expression of CB_1 receptor in proliferating GCPs (Fig. 1*C*, *arrowhead*). Differentiated cerebellar granule cells after 7 days in culture (DIV 7) showed an intense CB_1-membrane staining overlapping the N-CAM stain (Fig. 1*A*), which is consistent with a high expression of CB_1 receptors in differentiated neurons in the adult cerebellum (21). As expected, GCP cultures from CB_1-deficient mice (36) did not show immunostaining for the CB_1 receptor (Fig. 1*B*). Confirming the results obtained by CB_1 immunocytochemistry, RT-qPCR showed that CB_1 receptors were expressed in GCPs at DIV 1, even though their level of expression was lower (10 times less) compared with differentiated cerebellar granule cells at DIV 7 (Fig. 1*D*).

To further characterize the developmental pattern of CGPs in culture, we examined the expression of two genes, N-Myc and $GABA_A$ receptor, in cultures at DIV 1 and DIV 7. Although *N-myc* is a marker of proliferating GCPs (45), the *$GABA_A$* receptor is expressed by mature CGCs (46). Accordingly, we found that N-Myc mRNA expression was higher at DIV 1 that at DIV 7 and that the opposite occurred for $GABA_A$ receptor (Fig. 1*E*).

Because neural stem cells from the SVZ appear to express both CB_1 and CB_2 receptors (47), we wondered whether GCPs also express CB_2 receptors. We found CB_2 receptor transcripts were present in DIV 1 and DIV 7 granule cell cultures but at levels much lower than those of the CB_1 receptors (Fig. 1*D*). Although CB_2 receptor expression slightly increased from DIV 1 to DIV 7, it remained at a level that was 10^4 times lower than that of CB_1 receptors (Fig. 1*B*). Pharmacological studies suggest the existence of additional receptors for cannabinoids. For example, arachidonylethanolamide and the CB_1-selective antagonist rimonabant (SR141716A) bind to the TRPV1 vanilloid receptor, which is also named transient receptor potential vanilloid channel 1 (48). We found that no transcripts for TRPV1 were detectable in either DIV 1 or DIV 7 granule cell cultures (data not shown). Based on the low expression levels of the CB_2 receptors and absence of TRPV1 receptors, cannabinoids should act on GCPs mainly through CB_1 receptors.

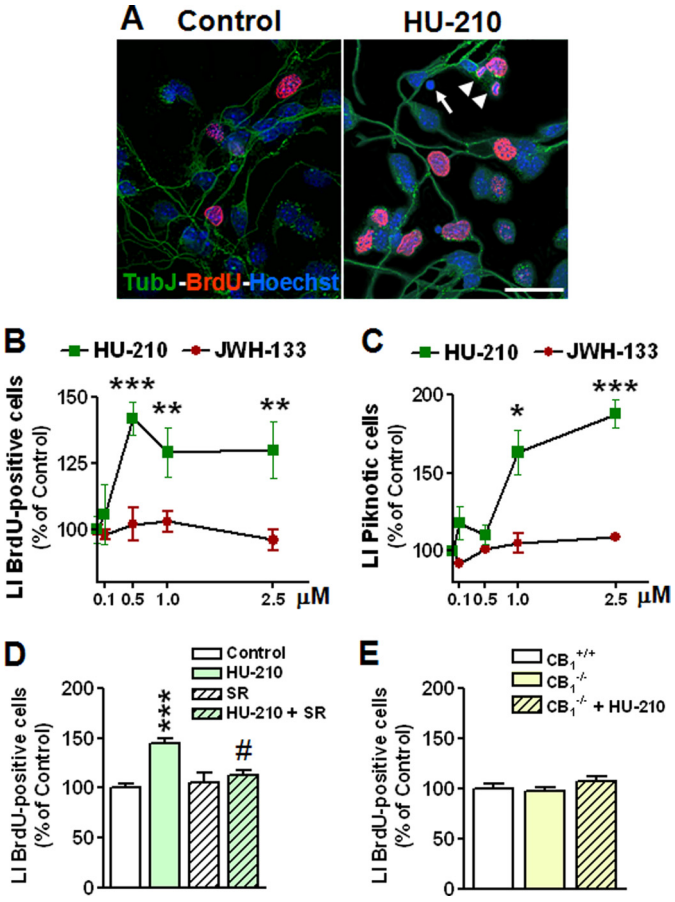

FIGURE 2. **Effect of HU-210 on proliferation/survival of cultured GCPs.** *A*, 1 h after plating cultures of GCPs were stimulated with HU-210 (0.5 μM) for 20 h. BrdUrd (10 μM) was added for the last 6 h and thereafter cells were processed for double immunofluorescence with anti-BrdUrd (*red*) and anti-β-tubulin III (TubJ, *green*) antibodies. Cell nuclei were stained by Hoechst dye (*blue*). The *arrow* indicates a pyknotic nucleus; the *arrowheads* indicate condensed mitotic chromosomes of a BrdUrd-positive cell. *Scale bar*: 30 μm. *B*, labeling index (*LI*), defined as percentage of BrdUrd-positive cells over the total cell number, was determined for GCP (DIV 1) treated with different doses of HU-210 (0.1, 0.5, 1, and 2.5 μM) or JWH-133 (0.1, 0.5, 1, and 2.5 μM). *C*, percentage of apoptotic GCPs over the total cell number in cultures treated as reported in *B*. Apoptotic cells were evaluated by counting pyknotic Hoechst-stained nuclei. Data (*B* and *C*) are expressed as the mean ± S.E. of four independent experiments. The *asterisks* indicate a significant difference between the treated *versus* untreated condition; *, $p < 0.05$; **, $p < 0.01$; ***, $p < 0.001$ (Bonferroni test after ANOVA). *D*, LI was determined in cultures untreated (control) or treated with HU-210 (0.5 μM), SR141716A (2.0 μM, SR), and HU-210 plus SR141716A. *Bars* are the mean ± S.E. of four independent experiments. ***, $p < 0.001$, treated *versus* control (untreated) condition; #, $p < 0.01$ HU-210 plus SR *versus* HU-210-only-treated cells (Bonferroni test after ANOVA). *E*, LI of BrdUrd-positive cells in cultures generated from CB_1-deficient mice ($CB_1^{-/-}$) and $CB_1^{+/+}$-treated or untreated with HU-210 (0.5 μM). *Bars* are the mean ± S.E. of three independent experiments.

Activation of the CB_1 Receptor Increases Proliferation of Cerebellar Granule Precursors—To test whether CB_1 and/or CB_2 receptor agonists affect GCP proliferation, we determined the effects of different concentrations of HU-210 (a CB_1 and CB_2 agonist) and JWH-133 (a CB_2-selective agonist) on proliferation of GCPs. Cell proliferation was evaluated through BrdUrd immunohistochemistry. Under control conditions, proliferating GCPs represented ~8–10% of total cell number. In cultures treated with HU-210 for 24 h, the number of proliferating cells increased up to 40–50% at concentrations of 0.5–2.5 μM (Fig. 2*B*). By contrast, treatment with JWH-133 had no effect on cell proliferation even at the highest tested concentration (Fig. 2*B*), suggesting that the effect of HU-210 on cell proliferation was specifically mediated by CB_1 receptors.

Because there is evidence that the activation of CB_1 receptors in differentiated granule cells induces apoptotic cell death (24), we counted the number of apoptotic cells in cultures treated either with HU-210 or JWH-133. Apoptotic cells were recognized based on the pyknotic appearance of Hoechst-stained nuclei (*white arrow* in Fig. 2*A*). Under control conditions, apoptotic cells represented ~6–7% of total cell number. HU-210 induced an increase in apoptotic cell death (up to +70 and 90%) at the two highest tested concentrations (1.0 and 2.5 μM) (Fig. 2*C*) but at the concentration of 0.5 μM HU-210 did not modify cell death (Fig. 2*C*). Similar results were obtained by evaluating the number of dying cells based on Trypan blue staining (data not shown). Because treatment with 0.5 μM HU-210 notably increased GCP proliferation without affecting cell death, subsequent cell culture experiments were performed in the presence of 0.5 μM HU-210.

To confirm that the increase in GCP proliferation was specifically due to CB_1 activation, we used SR141716A (rimonabant), a selective antagonist of CB_1 receptors. GCPs were incubated with SR141716A (2 μM) for 24 h alone or in the presence of HU-210. As shown in Fig. 2, while treatment with SR141716A alone was ineffective on GCP proliferation, the effect of HU-210 on GCP proliferation was prevented by co-treatment with SR141716A (Fig. 2*D*). To confirm that activation of CB_1 receptors is necessary to induce an increase in GCP proliferation, we generated GCP cultures from CB_1-deficient mice (36) and their wild-type littermates. We found that HU-210 was unable to increase GCP proliferation in CB_1-deficient neuronal progenitors (Fig. 2*E*), supporting the direct impact of CB_1 receptor activation on GCP proliferation.

Intracellular Signaling Involved in HU-210-induced Cerebellar Granule Precursor Proliferation—The phosphatidylinositol 3-kinase (PI3K)/AKT signaling plays a role in self-renewal of neural stem cells (49) and can mediate mitogenic signaling during corticogenesis (50). Because cannabinoids appear to regulate cell proliferation of oligodendrocytes and neuronal precursors via $G_{i/o}$, PI3K, and AKT (34, 47), we sought to establish whether this pathway is involved in the CB_1-mediated regulation of GCP proliferation.

We first analyzed the phosphorylation of AKT and its downstream target, the glycogen synthase kinase-3β (GSK-3β) (51) by Western blot analysis. AKT is activated by phosphorylation of two critical residues, namely threonine 308 and serine 473 (52). We found that HU-210 increased phosphorylation of AKT, at both Thr-308 and Ser-473 residues, and of GSK-3β and that this action was prevented by the PI3K inhibitor wortmannin (Fig. 3, *A–C*). Wortmannin treatment by itself reduced AKT Thr-308 and Ser-473 and GSK-3β phosphorylation, suggesting that basal AKT and GSK-3β phosphorylation in this cell system mainly depends on PI3K. We evaluated the number of BrdUrd-positive GCPs in the presence of wortmannin plus HU-210 and found that HU-210 was unable to increase cell proliferation when PI3K was inhibited (Fig. 3*D*). We found that exposure to wortmannin alone slowed down GCP proliferation rate, which was decreased by ~20%, as compared with un-

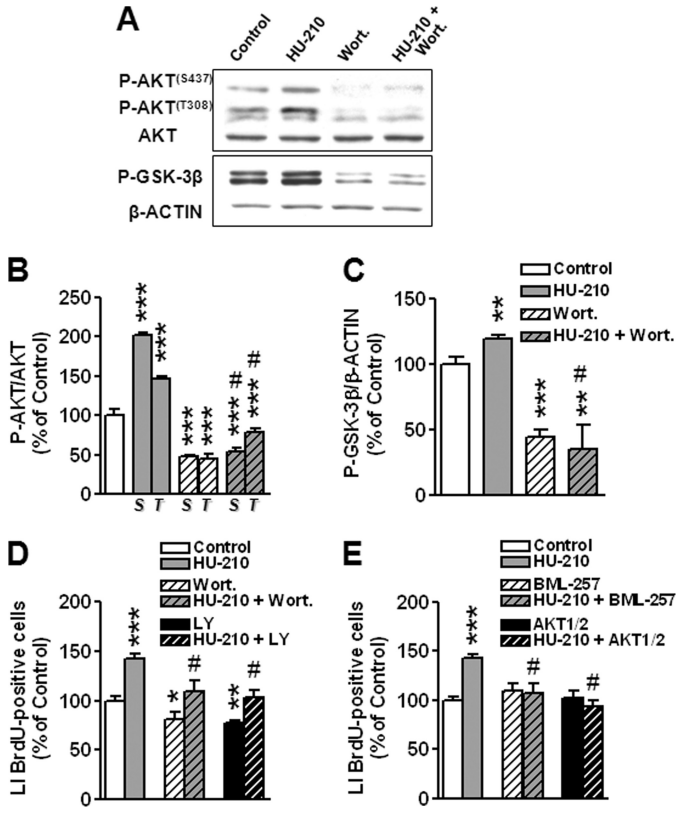

FIGURE 3. **Effects of HU-210 on PI3K/AKT/GSK-3β signaling of cultured GCPs.** *A*, examples of immunoblotting with anti-AKT, anti-phospho-AKT-Thr^{308}, anti-phospho-AKT-Ser^{473}, anti-phospho-GSK-3β-Ser^{9} and anti-β-actin antibodies obtained from total GCP extracts. Cultures of GCP at DIV 1 were stimulated for 1.5 h with HU-210 (0.5 μM), wortmannin (*Wort*, 100 nM), HU-210 plus wortmannin. *B* and *C*, P-AKT-Ser^{473} (*S*), P-AKT-Thr^{308} (*T*) (*B*) and P-GSK-3β (*C*) protein levels were normalized, respectively, to total AKT and β-actin content and expressed as percentage of untreated condition (100%). *D*, LI was determined for GCPs treated as reported in *A* or treated with either a selective PI3K inhibitor, LY294002 (*LY*; 10 μM) or HU-210 plus LY294002. *E*, LI was determined for GCPs treated with HU-210 (0.5 μM), BML-257 (12.5 μM), HU-210 plus BML-257, Akti-1/2 (60 nM), or HU-210 plus Akti-1/2 for 1.5 h. *Bars* are the mean ± S.E. of four experiments. *, $p < 0.05$; **, $p < 0.01$; ***, $p < 0.001$ as compared with control (untreated) condition; #, $p < 0.05$ as compared with corresponding HU-210-treated samples (Bonferroni test after ANOVA).

treated cells (Fig. 3*D*). Similar results were obtained using another selective PI3K inhibitor LY294002 (Fig. 3*D*). These data clearly show that CB_1 receptors exert their effects on proliferation through PI3K. We analyzed the effect of two inhibitors of AKT, BML-257, an inhibitor of AKT membrane translocation (53), and Akti-1/2, a selective non-ATP-competitive inhibitor (54), on HU-210-induced GCP proliferation. We found that both inhibitors completely blocked the effect of HU-210 on GCP proliferation (Fig. 3*E*). These data show that cannabinoids exert their effects on GCP proliferation through the PI3K/AKT pathway.

Because the mitogen-activated protein kinase/extracellular signal-regulated protein kinase (ERK) pathway appears to be modulated by cannabinoids in hippocampal neuronal precursors (20), we examined the possibility that in GCPs CB_1 activation affects the phosphorylation levels of ERK1/2. We found that HU-210 administration did not modify the phosphorylation levels of ERK1/2 detected by immunoblot (data not shown), indicating that ERK is not involved in the cannabinoid effect on GCP proliferation.

There is evidence that CB_1 receptors can interact with the receptor tyrosine kinase signaling (55). Mechanisms for CB_1 receptor-receptor tyrosine kinase transactivation include cleavage of membrane-bound precursor proteins such as EGF (55). We found that treatment with PD158780, a selective EGF receptor inhibitor, did not reduce the HU-210-induced GCP proliferation (data not shown), suggesting that transactivation of the EGF pathway is not involved in the CB_1-induced cell proliferation.

HU-210 Induced β-Catenin Accumulation through PI3K/AKT Activation—In the mitogenic signaling pathways Wnt and fibroblast growth factor-2, the phosphorylation-induced inactivation of GSK-3β leads to nuclear translocation of β-catenin (56, 57). In the nucleus, β-catenin binding to TCF/LEF converts these transcriptional repressors into activators and results in up-regulation of a variety of genes important in a wide variety of developmental events (58).

GCPs treated with HU-210 for 1.5 h showed an increase in β-catenin immunoreactivity in the nuclear compartment (Fig. 4*A*). Quantification of β-catenin protein levels in the nuclear fraction showed an increase by ~100% following HU-210 treatment (Fig. 4*B*). Co-treatment with BML-257 completely prevented the effect of HU-210 on β-catenin nuclear accumulation (Fig. 4*B*), suggesting the involvement of AKT in β-catenin nuclear translocation. In the nucleus β-catenin interacts with transcription factors of the LEF/TCF family to induce changes in the expression of cell-cycle genes, such as *cyclin D1* (59). Consistent with this, we found that cyclin D1 mRNA expression was significantly increased in GCPs after HU-210 treatment (Fig. 4*C*).

To define whether *β-catenin* is an essential gene by which CB_1 induces GCP proliferation, in cultures of GCPs, we suppressed its expression with antisense oligonucleotides (AS), using sense oligonucleotides (S) as control (41). We found that 24-h treatment with AS but not with S markedly decreased the expression of β-catenin in a dose-dependent manner (Fig. 4*D*). We then evaluated GCP proliferation after 24 h of co-treatment with HU-210 and different concentrations of AS or S. Co-treatment with AS, but not with S, completely blocked the effect of HU-210 on GCP proliferation (Fig. 4*E*), indicating the involvement of β-catenin in the cannabinoid effect on GCP proliferation.

To establish whether the CB_1-dependent activation of the AKT/GSK-3β/β-catenin system, observed in GCPs, is also present in other neuronal precursor types, we used clonally expanded neurospheres derived from neuronal precursors from the SVZ of newborn mice. As previously reported (18), we found that HU-210 increased neurosphere generation (data not shown) and neuronal precursor proliferation (Fig. 5*A*). The effect of CB_1 activation on nuclear accumulation of β-catenin was subsequently examined. Treatment with HU-210 for 1.5 h increased the nuclear accumulation of β-catenin (Fig. 5, *B* and *C*) up to 60% (Fig. 5*D*). This effect was completely prevented by the selective CB_1 antagonist SR141716A (Fig. 5*D*), ruling out the involvement of the CB_2 receptors or other nonspecific mechanisms. To explore the mechanism by which HU-210 induces β-catenin nuclear translocation in precursors from the SVZ, we examined whether nuclear translocation of β-catenin

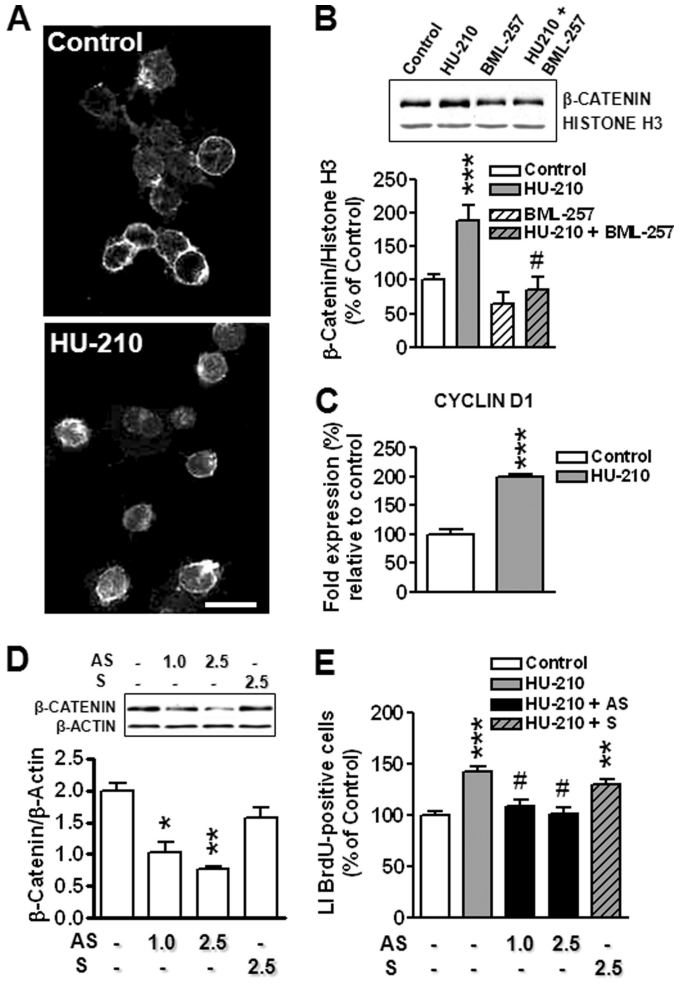

FIGURE 4. **HU-210 induces nuclear translocation of β-catenin in cultured GCPs.** *A*, images of cultured GCPs either untreated or treated with HU-210 for 1.5 h. β-Catenin localization was detected by immunofluorescence with an anti-β-catenin antibody. *Scale bar*: 10 μm. *B*, representative examples of Western blots probed with an anti-β-catenin monoclonal antibody. Nuclear fractions of protein lysates were isolated from GCPs untreated or treated with HU-210 (0.5 μM), BML-257 (12.5 μM), or HU-210 plus BML-257. Analysis of β-catenin levels in nuclear fractions was performed by immunoblotting. Values represent the percentage increase with respect to unstimulated cells (100% control value) and were obtained by normalization of densitometric values of β-catenin with respect to histone H3. *Bars* are the mean ± S.E. of three experiments. ***, $p < 0.001$ as compared with control (untreated) condition; #, $p < 0.05$ as compared with corresponding HU-210-treated samples (Bonferroni test after ANOVA). *C*, cyclin D1 expression quantified by RT-qPCR, in cultures of GCPs at DIV 1 treated with HU-210 (1.0 μM) for 24 h. Data are expressed as mean ± S.E. of three experiments. ***, $p < 0.001$ (Bonferroni test after ANOVA). *D*, Western blots analysis of β-catenin levels in total protein extracts of GCPs treated for 24 h with antisense β-catenin oligonucleotides (AS, 1 μM, 2.5 μM). Sense β-catenin oligonucleotides (*S*, 2.5 μM) were used as control. Values represent β-catenin levels normalized with respect to β-actin. *Bars* are the mean ± S.E. of three experiments. *, $p < 0.05$; **, $p < 0.01$; ***, $p < 0.001$ as compared with untreated condition (Bonferroni test after ANOVA). *E*, LI was determined for GCPs untreated (control) and treated for 24 h with either HU-210 (0.5 μM) or HU-210 plus different concentrations of AS or S oligonucleotides. *Bars* are the mean ± S.E. of four experiments. **, $p < 0.01$; ***, $p < 0.001$ as compared with control (untreated) condition; #, $p < 0.05$ as compared with HU-210-treated sample (Bonferroni test after ANOVA).

was dependent on AKT signaling. To this purpose, we co-treated neurospheres with BML-257 and HU-210. BML-257 completely inhibited the nuclear translocation of β-catenin (Fig. 5*D*), indicating that in precursors from the SVZ CB_1-induced nuclear translocation of β-catenin was also mediated by the AKT signaling pathway.

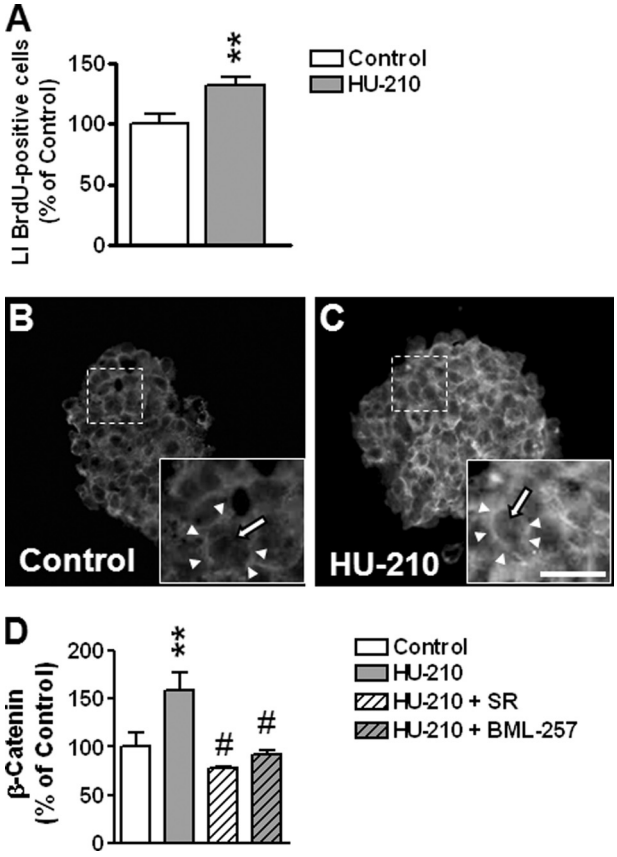

FIGURE 5. **Nuclear β-catenin accumulation through HU-210-mediated AKT activation in neurosphere cultures.** *A*, LI was determined for cultures of neurospheres (at passages 3–4) untreated or treated with HU-210 (0.5 μM). Values represent the percentage increase with respect to untreated cells (100% control value). *B* and *C*, images of neurospheres untreated (*B*) or treated (*C*) with HU-210 for 1.5 h. β-Catenin sub-cellular localization was detected by immunofluorescence with an anti-β-catenin antibody. The regions enclosed by a *square* are shown at a higher magnification at the *bottom*. Note the nuclear localization (nucleus is indicated by the *thin arrow*) of β-catenin in neurospheres treated with HU-210. *Arrowheads* indicate the perinuclear β-catenin localization. *Scale bar*: 40 μm (medium magnifications); 15 μm (high magnifications). *D*, nuclear β-catenin levels were quantified by immunofluorescence intensity (as described under "Experimental Procedures") of neurosphere cultures untreated or treated with HU-210 (0.5 μM), HU-210 plus SR141716A (2.0 μM, SR), or HU-210 plus BML-257 (12.5 μM). Values represent the percentage increase with respect to unstimulated cells (100% control value). *Bars* (*A* and *D*) are the mean ± S.E. of three experiments. **, $p < 0.01$ as compared with control (unstimulated) condition; #, $p < 0.05$ as compared with corresponding HU-210-treated samples (Bonferroni test after ANOVA).

HU-210 Promotes Cerebellar Granule Precursor Proliferation during Cerebellar Development—In mouse cerebellum, the production of granule neurons lasts from birth to the second postnatal week, with a peak during the first postnatal week (60). Newborn cells derive from GCPs located in the EGL. The EGL can be subdivided into two morphologically distinct zones, the outer EGL (oEGL) (Fig. 6, *A* and *B*), which is formed by actively dividing GCPs, and the inner EGL (iEGL) (Fig. 6, *A* and *B*), which mainly contains pre-migratory postmitotic cells (61, 62).

To confirm results obtained in culture, we dissected by the laser capture technique the oEGL from the cerebellum of P6 mouse pups and analyzed CB_1 expression by qRT-PCR. We found that CB_1 receptors were expressed by GCPs located in the oEGL (Fig. 6*C*). The expression levels were lower than in whole cerebellar extracts (Fig. 6*C*), which is in line with the

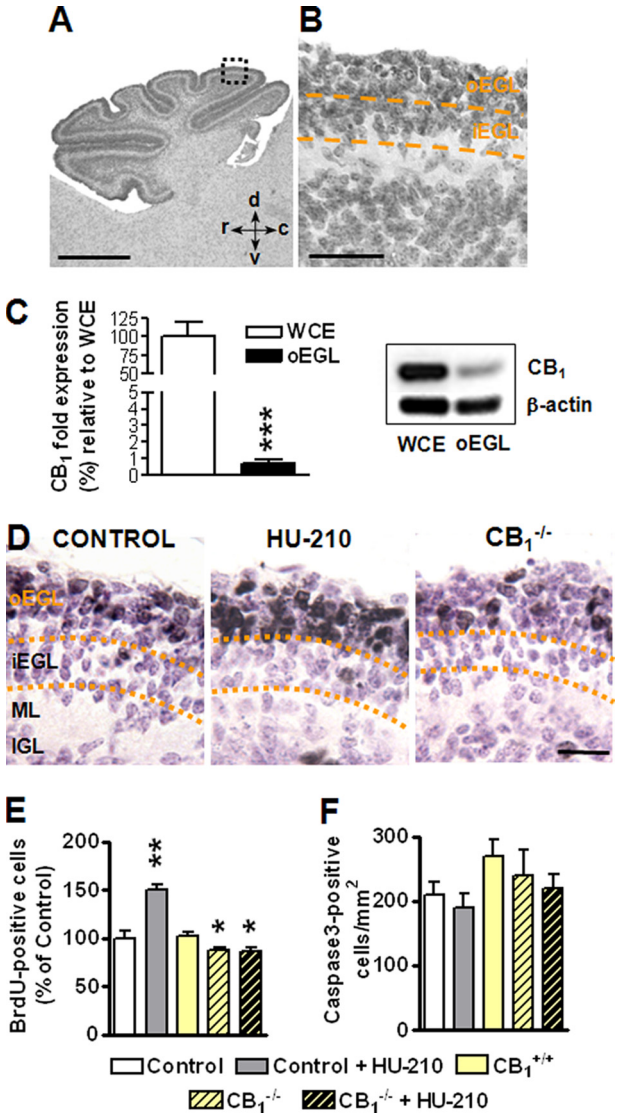

FIGURE 6. **Effects of HU210 treatment on GCP proliferation during postnatal cerebellar development.** *A*, example of a sagittal Nissl-stained section across the cerebellum of a P6 mouse. *Scale bar*: 200 μm. *B*, high magnification photomicrograph of the region enclosed by a *square* in *A* showing the cerebellar layers. The *dashed lines* indicate the borders of the oEGL and iEGL. *Scale bar*: 50 μm. *C*, quantification by RT-qPCR of CB_1 receptor expression in extracts from the whole cerebellum (*WCE*) and from the oEGL microdissected with the laser capture technique (see "Experimental Procedures") of P6 mouse pups. An example of amplicons resolved on acrylamide is shown on the *right*. Data, given as % of CB_1 expression in whole cerebellar extracts, are expressed as the mean ± S.E. ***, $p < 0.001$ (two-tailed *t* test). *D–F*, C57BL/6J, $CB_1^{+/+}$, and $CB_1^{-/-}$ mice received two subcutaneous injections either of phosphate-buffered saline (control) or HU-210 (100 μg/kg) for 3 days, starting at P4. Mice received one BrdUrd injections on P6 and were sacrificed after 2 h. Examples of sections immunostained for BrdUrd and counterstained with hematoxylin and eosin (*D*). Cells with brown nuclei are BrdUrd-positive cells. The *dashed lines* indicate the borders of the oEGL and iEGL. *Scale bar*: 25 μm. Quantification of BrdUrd-positive cells in the cerebellum of untreated ($n = 5$) or HU-210-treated ($n = 5$) C57BL/6J mice, untreated ($n = 4$) or HU-210-treated ($n = 3$) $CB_1^{+/+}$ mice, and untreated ($n = 3$) or HU-210-treated ($n = 3$) $CB_1^{-/-}$ mice (*E*). BrdUrd-positive cells were counted in the EGL and were expressed as percentage of BrdUrd positive cells/mm^2 relative to control mice. Density of cleaved caspase-3-positive cells (*F*) in the cerebellum of the mice reported in *E*. *, $p < 0.05$; **, $p < 0.01$; ***, $p < 0.001$ (Bonferroni test after ANOVA). *c*, caudal; *d*, dorsal; *iEGL*, inner external granular layer; *IGL*, internal granular layer; *ML*, molecular layer; *oEGL*, outer external granular layer; *r*, rostral; and *v*, ventral.

lower levels of CB_1 receptors found *in vitro* in undifferentiated (DIV 1) *versus* differentiated (DIV 7) granule cells (Fig. 1, *A* and *D*).

To establish whether activation of CB_1 receptors during cerebellar development induces an increase in neuronal proliferation similar to that observed *in vitro*, mouse pups were injected with vehicle or HU-210 (100 μg/kg, intraperitoneal; two daily injections for 3 days). To evaluate cell proliferation, animals received one BrdUrd injection at the end of treatment. Two hours after BrdUrd injection, most of the BrdUrd-positive cells were located in the oEGL and only scattered BrdUrd-positive cells were present in the iEGL (Fig. 6*D*). Estimate of the density of BrdUrd-positive cells in the EGL showed that HU-210-treated mice had more (+50%) BrdUrd-positive cells than control mice (Fig. 6, *D* and *E*).

The $CB_1^{-/-}$ mouse is an ideal model to test the role of the endocannabinoid/CB_1 system on GCP proliferation. To establish the physiological role of this system we compared granule cell proliferation in neonate $CB_1^{-/-}$ mice and wild-type littermates. We found that in mice without CB_1 receptors GCP proliferation was significantly smaller (−18%) than in wild-type littermates (Fig. 6, *D* and *E*), indicating that the endocannabinoid system is physiologically involved in regulation of GCP during cerebellar development. HU-210 treatment in neonate $CB_1^{-/-}$ mice had no effect on GCP proliferation (Fig. 6*E*), confirming that the CB_1 receptor is involved in the HU-210-promoted neuronal proliferation.

Because there is evidence that cannabinoid administration increases apoptotic cell death (63), we counted the number of apoptotic cells in the cerebellum of HU-210-treated and untreated mice. Apoptotic cells were recognized based on cleaved caspase-3 immunostaining. At this stage of development, there were very few apoptotic cells in both the EGL and IGL of untreated mice. Estimate of the density of apoptotic cells in these two layers showed no significant differences between HU-210-treated and untreated mice (Fig. 6*F*), indicating that the dose of HU-210 used here has no adverse effects on cell survival. No differences were found in apoptotic cell death among $CB_1^{-/-}$, HU-210-treated $CB_1^{-/-}$ mice, and wild-type littermates (Fig. 6*F*), suggesting that lack of the CB_1 receptor does not compromise cell survival.

Activation of the CB_1 Receptor in Vivo Promotes β-Catenin Nuclear Translocation in Cerebellar Granule Precursors through the AKT/GSK-3β Pathway—To establish whether CB_1 receptors activate the AKT/GSK-3β pathway also *in vivo*, the levels of p-AKT (Ser^{473}) and p-GSK-3β were quantified by Western blot, in cerebellar homogenates (Fig. 7*A*), and visualized by immunostaining, in cerebellar sections (Fig. 7, *B* and *C*), from HU-210-treated and untreated mice. We found an increase in the phosphorylation levels of both AKT and GSK-3β (Fig. 7, *A–C*), which confirms results obtained *in vitro*.

We then analyzed β-catenin expression and found that it was considerably higher in cerebellar extracts from mice treated with HU-210 with respect to untreated mice (Fig. 7*D*). To examine more in detail the increase of β-catenin at the cellular level, cerebellar sections were immunostained with a β-catenin antibody (Fig. 7, *E* and *F*). We found that β-catenin expression was considerably higher in the EGL of mice treated with

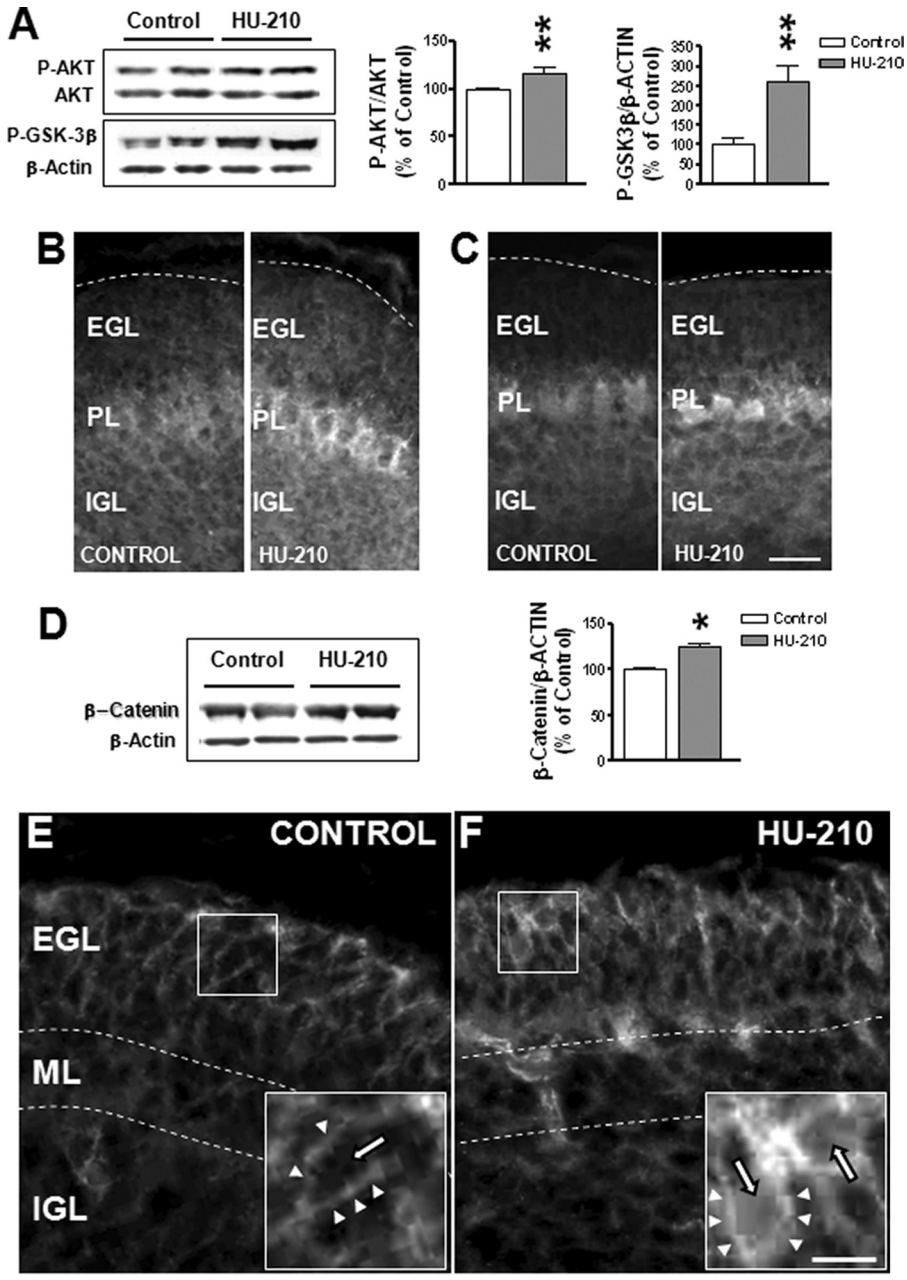

FIGURE 7. **Effect of HU-210 on AKT and GSK-3β phosphorylation and β-catenin nuclear translocation during postnatal cerebellar development.** *A*, examples of immunoblotting with anti-phospho-AKT-Ser^{473} and anti-phospho-GSK-3β-Ser^{9} antibodies obtained from total cerebellar extracts of P6 untreated and HU-210-treated mice. Protein levels were normalized to total AKT or β-actin content, respectively, and expressed as percentage of untreated condition. *Bars* are the mean ± S.E. of three experiments. *, $p < 0.05$; **, $p < 0.01$, treated *versus* untreated condition (Bonferroni test after ANOVA). *B* and *C*, photomicrographs of sagittal sections immunostained for phospho-AKT-Ser^{473} (*B*) and phospho-GSK-3β-Ser^{9} (*C*) across the cerebellum of a P6 control and HU-210-treated mouse. *Dashed lines* indicate the outer borders of the external granular layer. *Scale bar*: 20 μm. *D*, representative example of a Western blot (same cerebellar extracts as in *A*) probed with an anti-β-catenin antibody. Protein levels were normalized to total β-actin content and expressed as percentage of untreated condition. *Bars* are the mean ± S.E. of three experiments. *, $p < 0.05$ treated *versus* untreated condition (Bonferroni test after ANOVA). *E* and *F*, photomicrographs of sagittal sections immunostained for β-catenin across the cerebellum of a P6 untreated (*E*) and HU-210-treated mouse (*F*). The regions enclosed by a *square* are shown at a higher magnification at the *bottom*. Note that in the EGL of untreated animals (*E*), β-catenin had mainly an extranuclear location (*arrowheads*), whereas in HU-210-treated animals (*F*) it was present both at the nuclear (*white arrow*) and extranuclear level (*arrowheads*). *Dashed lines* indicate the borders of the cerebellar layers. The *scale bar*: 40 μm (medium magnifications); 20 μm (high magnifications) applies to *E* and *F*. *EGL*, external granular layer; *IGL*, internal granular layer; *ML*, molecular layer; and *PL*, Purkinje cell layer.

HU-210 (Fig. 7*F*) compared with untreated mice (Fig. 7*E*), which is in agreement with the increased phosphorylation levels of GSK-3β in treated mice. Although in untreated animals β-catenin had mainly an extranuclear location (Fig. 7*E*), in HU-210-treated mice it was present both at the nuclear and extranuclear level (Fig. 7*F*, *arrows*).

DISCUSSION

The process of neurogenesis is modulated by numerous neurobiological factors, including the endocannabinoid system (15–20). Although it is well established that the endocannabinoid system is involved in the modulation of precursor proliferation in the hippocampus and VZ/SVZ, it is presently unknown whether it may exert a more widespread action during brain development, modulating the proliferation of neuronal precursors in various brain neurogenic regions. Moreover, very little is known about the molecular mechanisms by which endocannabinoids modulate neuronal precursor proliferation. Our results demonstrate that cannabinoids modulate proliferation also of cerebellar neuronal precursors, via the CB_1 receptor. Our study additionally shows that, in neuronal precursors from both the cerebellum and SVZ, CB_1 receptors promote proliferation through the PI3K/AKT/GSK-3β/β-catenin pathway, suggesting that this pathway plays a pivotal role in the CB_1-dependent modulation of neuronal proliferation.

CB_1 Receptors Are Expressed by Cerebellar Granule Cell Precursors and Their Activation Promotes Proliferation—CB_1 immunoreactivity is abundant in the adult cerebellum (21), where CB_1 receptors reside primarily in the presynaptic terminals of parallel fibers arising form granule cells located in the internal granular layer (21). Here we addressed the question whether cannabinoid receptors are expressed by the precursors of cerebellar granule cells. We report, for the first time, that GCPs express CB_1 receptors, similarly to the precursors of the hippocampus and VZ/SVZ (15–20). CB_2 receptors appear to be expressed by differentiated cerebellar granule cells, though at a lower level than CB_1 receptors (64). This is in agreement with our finding of very low levels of CB_2 receptors in cultures of granule cells (see Fig. 1*B*).

Administration of HU-210, a potent agonist of CB_1 and CB_2 receptors, increased GCP proliferation rate. This effect was mediated by CB_1 receptors, because it was prevented by co-treatment with SR141716A, a selective CB_1 receptor antagonist. This conclusion is strengthened by the observation that in CB_1-deficient mice treatment with HU-210 was unable to increase GCP proliferation. Although CB_2 receptors have been recently described to promote proliferation of neural stem cells derived from the cortex of mouse embryos (47), we found that a CB_2-selective agonist did not affect GCP proliferation. Taken together these data suggest that the cannabinoid system regulates GCP proliferation through CB_1 receptors.

The fact that GCP proliferation, neither in $CB_1^{-/-}$ granule cultures nor in control cultures treated with SR141716A, was impaired suggests that endocannabinoid production is a non-cell-autonomous process for cerebellar granule cell precursors.

CB_1 Receptors Modulate Cerebellar Granule Precursor Proliferation through the PI3K/AKT/GSK-3β/β-Catenin Pathway—We found that HU-210 treatment increased phosphorylation of AKT and GSK-3β and that inhibition of PI3K and AKT suppressed the CB_1-mediated proliferation increase of GCPs. These data indicate the involvement of the PI3K/AKT/GSK-3β pathway in regulation of GCP proliferation. Our results are in agreement with evidence in other cellular systems, showing that cannabinoids regulate cell proliferation of oligodendrocytes and cortical neuronal precursors via $G_{i/o}$, PI3K, and AKT (34, 47). We found that ERK phosphorylation levels did not change following activation of CB_1 receptors, suggesting that this kinase is not involved in the CB_1-mediated regulation of GCP proliferation. The CB_1-dependent proliferation increase of embryonic hippocampal neuronal precursors requires ERK activation (20), suggesting that the pro-proliferative pathways downstream from CB_1 receptors may include ERK in some types of precursor cells.

β-Catenin, an important mediator of the canonical Wnt-signaling pathway (56, 65) is a multifunctional protein, the stability of which is mainly regulated by GSK-3β. This is consistent with our results showing that increased phosphorylation of GSK-3β was accompanied by increased levels of β-catenin within the nuclear compartment. The observation that inhibition of AKT prevented β-catenin nuclear translocation following HU-210 treatment suggests that β-catenin belongs to a CB_1 receptor-driven signaling pathway formed by PI3K/AKT/GSK-3β/β-catenin.

When phosphorylated by GSK-3β, β-catenin is ubiquitinated and becomes degraded by the proteasome pathway. When GSK-3β is inactivated through phosphorylation, β-catenin is stabilized and accumulates in the cytosol and can be translocated to the nucleus where it functions as a transcriptional regulator (66, 67). Recent evidence shows that β-catenin, besides being involved in a variety of functions (68, 69), plays an important role in regulating proliferation of neural stem cells. In these cells, β-catenin acts downstream from the canonical Wnt-signaling pathway (65, 70–72) and appears to increase proliferation by decreasing cell cycle exit (71). A recent study suggests that fibroblast growth factor-2 regulates neural stem cell proliferation via β-catenin signaling (73). The finding that inhibition of β-catenin expression prevented the CB_1-induced proliferation increase of GCPs indicates that β-catenin regulates proliferation of GCPs by acting downstream from a cannabinoid-signaling pathway. This mechanism appears to be shared by different types of neuronal precursors, because β-catenin nuclear translocation following activation of CB_1 receptors was present not only in GCPs but also in neuronal precursors derived from SVZ. Our data additionally suggest that cyclin D1 up-regulation may be one of the mechanisms by which β-catenin regulates proliferation of neuronal precursors.

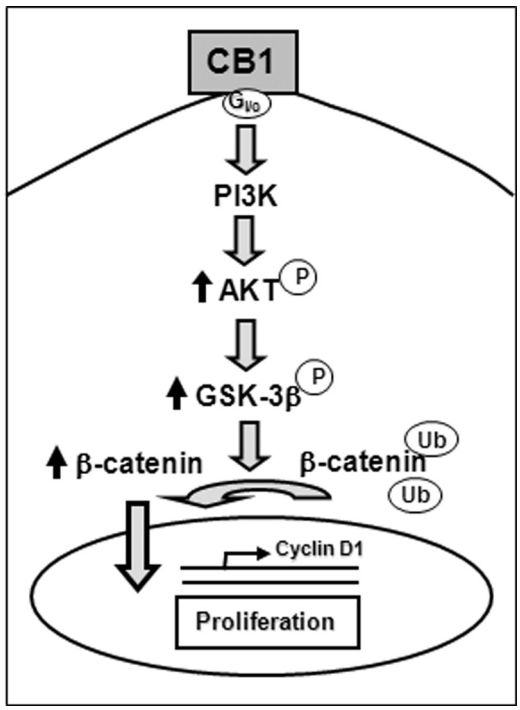

FIGURE 8. **Schematic drawing summarizing the signaling pathway downstream from CB_1 receptors in cerebellar granule cell precursors.** Cannabinoids induce neuronal proliferation by CB_1 signaling via PI3K/AKT activation, GSK-3β inactivation, and β-catenin nuclear translocation.

Taken together, our results suggest a plausible mechanism for the regulation of neuronal precursor proliferation by cannabinoids, via β-catenin. As summarized by Fig. 8, CB_1 receptor activation increases PI3K/AKT activity. Following AKT-mediated phosphorylation of GSK-3β, β-catenin is stabilized and translocates to the nucleus where it functions as a transcriptional regulator, modulating the expression of genes, such as *cyclin D1*, involved in the regulation of cell proliferation.

Role for the Endocannabinoid System on GCP Proliferation during Cerebellar Development—Current findings *in vivo* show that (i) HU-210 administration to neonate mice increased GCP proliferation, (ii) proliferation was impaired in $CB_1^{-/-}$ mice, and (iii) proliferation did not increase in $CB_1^{-/-}$ mice following HU-210 treatment. All these data indicate that the endocannabinoid system plays a role in the control of neuronal precursor proliferation during cerebellar development through CB_1 receptors. Previous studies show that endocannabinoid signaling is instrumental for cortical and hippocampal neurogenesis (16, 19). Our findings in the cerebellum are in agreement with these studies and additionally suggest that endocannabinoids may have a widespread effect in the regulation of brain development.

Concerning the impact of the endocannabinoid system on cerebellar development, our data show that granule cell proliferation was relatively mildly impaired in $CB_1^{-/-}$ mice (−18%), suggesting that, although this system physiologically contributes to the regulation of cerebellar neurogenesis, it may not be the major actor in this process. Yet, the finding that agonists of CB_1 receptors are able to powerfully increase neuronal precursor proliferation (Fig. 2, *A* and *B*) (15–20) appears of relevance in the context of brain pathophysiology, because it provides a rational basis for studies aimed at establishing whether CB_1 receptor agonists may be employed in brain pathologies characterized by defects in neurogenesis/neurodegeneration. In this connection, it seems important to note that in mice treated with HU-210 apoptotic cell death was not affected in the cerebellum (current study) and hippocampus (20), suggesting that agonists of cannabinoid receptors can be employed to increase neurogenesis without concomitant aversive effects on cell survival.

In conclusion, our results support the notion that endocannabinoids constitute a new group of lipid signaling cues involved in the control of neuronal precursor proliferation and show that they may participate in the control of neurogenesis during early phases of brain development.

Acknowledgments—We are grateful to Dr. Giovanni Marsicano for kindly supplying $CB_1^{-/-}$ mice. We are particularly grateful for advice and helpful comments to Dr. Uberto Pagotto.

REFERENCES

1. Matsuda, L. A., Lolait, S. J., Brownstein, M. J., Young, A. C., and Bonner, T. I. (1990) *Nature* **346,** 561–564
2. Munro, S., Thomas, K. L., and Abu-Shaar, M. (1993) *Nature* **365,** 61–65
3. Piomelli, D., Giuffrida, A., Calignano, A., and Rodríguez de Fonseca, F. (2000) *Trends Pharmacol. Sci.* 21, 218–224
4. Porter, A. C., and Felder, C. C. (2001) *Pharmacol. Ther.* **90,** 45–60
5. Di Marzo, V., Melck, D., Bisogno, T., and De Petrocellis, L. (1998) *Trends Neurosci.* **21,** 521–528
6. Mechoulam, R., Spatz, M., and Shohami, E. (2002) *Sci STKE 2002,* re5
7. Mechoulam, R., Hanus, L., and Martin, B. R. (1994) *Biochem. Pharmacol.* **48,** 1537–1544
8. Pertwee, R. G. (1997) *Pharmacol. Ther.* **74,** 129–180
9. Childers, S. R., and Breivogel, C. S. (1998) *Drug Alcohol Depend.* **51,** 173–187
10. Fernández-Ruiz, J., Berrendero, F., Hernández, M. L., and Ramos, J. A. (2000) *Trends Neurosci.* **23,** 14–20
11. Berrendero, F., Sepe, N., Ramos, J. A., Di Marzo, V., and Fernández-Ruiz, J. J. (1999) *Synapse* **33,** 181–191
12. Buckley, N. E., Hansson, S., Harta, G., and Mezey, E. (1998) *Neuroscience* **82,** 1131–1149
13. Glass, M., Dragunow, M., and Faull, R. L. (1997) *Neuroscience* **77,** 299–318
14. Fernández-Ruiz, J. J., Berrendero, F., Hernández, M. L., Romero, J., and Ramos, J. A. (1999) *Life Sci.* **65,** 725–736
15. Berrendero, F., García-Gil, L., Hernández, M. L., Romero, J., Cebeira, M., de Miguel, R., Ramos, J. A., and Fernández-Ruiz, J. J. (1998) *Development* **125,** 3179–3188
16. Jin, K., Xie, L., Kim, S. H., Parmentier-Batteur, S., Sun, Y., Mao, X. O., Childs, J., and Greenberg, D. A. (2004) *Mol. Pharmacol.* **66,** 204–208
17. Rueda, D., Navarro, B., Martinez-Serrano, A., Guzman, M., and Galve-Roperh, I. (2002) *J. Biol. Chem.* **277,** 46645–46650
18. Aguado, T., Monory, K., Palazuelos, J., Stella, N., Cravatt, B., Lutz, B., Marsicano, G., Kokaia, Z., Guzmán, M., and Galve-Roperh, I. (2005) *FASEB J.* **19,** 1704–1706
19. Mulder, J., Aguado, T., Keimpema, E., Barabás, K., Ballester Rosado, C. J., Nguyen, L., Monory, K., Marsicano, G., Di Marzo, V., Hurd, Y. L., Guillemot, F., Mackie, K., Lutz, B., Guzmán, M., Lu, H. C., Galve-Roperh, I., and Harkany, T. (2008) *Proc. Natl. Acad. Sci. U.S.A.* **105,** 8760–8765
20. Jiang, W., Zhang, Y., Xiao, L., Van Cleemput, J., Ji, S. P., Bai, G., and Zhang, X. (2005) *J. Clin. Invest.* **115,** 3104–3116
21. Sim-Selley, L. J. (2003) *Crit. Rev. Neurobiol.* **15,** 91–119
22. Tsou, K., Brown, S., Sañudo-Peña, M. C., Mackie, K., and Walker, J. M. (1998) *Neuroscience* **83,** 393–411
23. Behesti, H., and Marino, S. (2009) *Int. J. Biochem. Cell Biol.* **41,** 435–445
24. Pozzoli, G., Tringali, G., Vairano, M., D'Amico, M., Navarra, P., and Martire, M. (2006) *J. Neurosci. Res.* **83,** 1058–1065
25. Vallano, M. L., Beaman-Hall, C. M., Bui, C. J., and Middleton, F. A. (2006) *Neuropharmacology* **50,** 651–660
26. Brown, S. P., Safo, P. K., and Regehr, W. G. (2004) *J. Neurosci.* **24,** 5623–5631
27. Breivogel, C. S., Walker, J. M., Huang, S. M., Roy, M. B., and Childers, S. R. (2004) *Neuropharmacology* **47,** 81–91
28. Howlett, A. C. (1995) *Annu. Rev. Pharmacol. Toxicol.* **35,** 607–634
29. Bouaboula, M., Perrachon, S., Milligan, L., Canat, X., Rinaldi-Carmona, M., Portier, M., Barth, F., Calandra, B., Pecceu, F., Lupker, J., Maffrand, J. P., Le Fur, G., and Casellas, P. (1997) *J. Biol. Chem.* **272,** 22330–22339
30. Sánchez, C., Galve-Roperh, I., Rueda, D., and Guzmán, M. (1998) *Mol. Pharmacol.* **54,** 834–843
31. Liu, J., Gao, B., Mirshahi, F., Sanyal, A. J., Khanolkar, A. D., Makriyannis, A., and Kunos, G. (2000) *Biochem. J.* **346,** 835–840
32. Rueda, D., Galve-Roperh, I., Haro, A., and Guzmán, M. (2000) *Mol. Pharmacol.* **58,** 814–820
33. Galve-Roperh, I., Sánchez, C., Cortés, M. L., Gomez del Pulgar, T., Izquierdo, M., and Guzmán, M. (2000) *Nat. Med.* **6,** 313–319
34. Molina-Holgado, E., Vela, J. M., Arévalo-Martín, A., Almazán, G., Molina-Holgado, F., Borrell, J., and Guaza, C. (2002) *J. Neurosci.* **22,** 9742–9753
35. Ozaita, A., Puighermanal, E., and Maldonado, R. (2007) *J. Neurochem.* **102,** 1105–1114
36. Marsicano, G., Wotjak, C. T., Azad, S. C., Bisogno, T., Rammes, G., Cascio, M. G., Hermann, H., Tang, J., Hofmann, C., Zieglgänsberger, W., Di Marzo, V., and Lutz, B. (2002) *Nature* **418,** 530–534
37. Gallo, V., Ciotti, M. T., Coletti, A., Aloisi, F., and Levi, G. (1982) *Proc. Natl. Acad. Sci. U.S.A.* **79,** 7919–7923
38. Reynolds, B. A., and Weiss, S. (1992) *Science* **255,** 1707–1710
39. Weiss, S., Dunne, C., Hewson, J., Wohl, C., Wheatley, M., Peterson, A. C., and Reynolds, B. A. (1996) *J. Neurosci.* **16,** 7599–7609
40. Contestabile, A., Fila, T., Bartesaghi, R., and Ciani, E. (2005) *J. Biol. Chem.* **280,** 33541–33551
41. Li, J., Zhang, J. V., Cao, Y. J., Zhou, J. X., Liu, W. M., Fan, X. J., and Duan, E. K. (2005) *Biol. Reprod* **72,** 700–706
42. Bianchi, P., Ciani, E., Contestabile, A., Guidi, S., and Bartesaghi, R. (2009) *Brain Pathol.* **20,** 106–118
43. Contestabile, A., Fila, T., Bartesaghi, R., and Ciani, E. (2009) *Brain Pathol.* **19,** 224–237
44. Lowry, O. H., Rosebrough, N. J., Farr, A. L., and Randall, R. J. (1951) *J. Biol. Chem.* **193,** 265–275
45. Kenney, A. M., Cole, M. D., and Rowitch, D. H. (2003) *Development* **130,** 15–28
46. Zheng, T. M., Zhu, W. J., Puia, G., Vicini, S., Grayson, D. R., Costa, E., and Caruncho, H. J. (1994) *Proc. Natl. Acad. Sci. U.S.A.* **91,** 10952–10956
47. Molina-Holgado, F., Rubio-Araiz, A., García-Ovejero, D., Williams, R. J., Moore, J. D., Arévalo-Martín, A., Gómez-Torres, O., and Molina-Holgado, E. (2007) *Eur. J. Neurosci.* **25,** 629–634
48. Zygmunt, P. M., Petersson, J., Andersson, D. A., Chuang, H., Sørgård, M., Di Marzo, V., Julius, D., and Högestätt, E. D. (1999) *Nature* **400,** 452–457
49. Watanabe, S., Umehara, H., Murayama, K., Okabe, M., Kimura, T., and Nakano, T. (2006) *Oncogene* **25,** 2697–2707
50. Mairet-Coello, G., Tury, A., and DiCicco-Bloom, E. (2009) *J. Neurosci.* **29,** 775–788
51. Cross, D. A., Alessi, D. R., Cohen, P., Andjelkovich, M., and Hemmings, B. A. (1995) *Nature* **378,** 785–789

52. Vogt, P. K., Aoki, M., Bottoli, I., Chang, H. W., Fu, S., Hecht, A., Iacovoni, J. S., Jiang, B. H., and Kruse, U. (1999) *Cell Growth & Differ.* **10,** 777–784
53. Lundholt, B. K., Linde, V., Loechel, F., Pedersen, H. C., Møller, S., Praestegaard, M., Mikkelsen, I., Scudder, K., Bjørn, S. P., Heide, M., Arkhammar, P. O., Terry, R., and Nielsen, S. J. (2005) *J. Biomol. Screen.* **10,** 20–29
54. Lindsley, C. W., Zhao, Z., Leister, W. H., Robinson, R. G., Barnett, S. F., Defeo-Jones, D., Jones, R. E., Hartman, G. D., Huff, J. R., Huber, H. E., and Duggan, M. E. (2005) *Bioorg. Med. Chem. Lett.* **15,** 761–764
55. Dalton, G. D., Bass, C. E., Van Horn, C., and Howlett, A. C. (2009) *CNS Neurol. Disord. Drug Targets* **8,** 422–431
56. Cadigan, K. M., and Nusse, R. (1997) *Genes Dev.* **11,** 3286–3305
57. Shimizu, T., Kagawa, T., Inoue, T., Nonaka, A., Takada, S., Aburatani, H., and Taga, T. (2008) *Mol. Cell. Biol.* **28,** 7427–7441
58. Peifer, M., and Polakis, P. (2000) *Science* **287,** 1606–1609
59. Shtutman, M., Zhurinsky, J., Simcha, I., Albanese, C., D'Amico, M., Pestell, R., and Ben-Ze'ev, A. (1999) *Proc. Natl. Acad. Sci. U.S.A.* 96, 5522–5527
60. Altman, J. (1982) *Exp. Brain Res. Suppl.* **6,** 8–49
61. Koppel, H., and Lewis, P. D. (1983) *Neuropathol. Appl. Neurobiol.* **9,** 207–214
62. Mares, V., and Lodin, Z. (1970) *Brain Res.* **23,** 343–352
63. Downer, E. J., Gowran, A., and Campbell, V. A. (2007) *Brain Res.* **1175,** 39–47
64. Skaper, S. D., Buriani, A., Dal Toso, R., Petrelli, L., Romanello, S., Facci, L., and Leon, A. (1996) *Proc. Natl. Acad. Sci. U.S.A.* **93,** 3984–3989
65. Zechner, D., Fujita, Y., Hülsken, J., Müller, T., Walther, I., Taketo, M. M., Crenshaw, E. B., 3rd, Birchmeier, W., and Birchmeier, C. (2003) *Dev. Biol.* **258,** 406–418
66. Dominguez, I., and Green, J. B. (2001) *Dev. Biol.* **235,** 303–313
67. Grimes, C. A., and Jope, R. S. (2001) *Prog. Neurobiol.* **65,** 391–426
68. Moon, R. T., Kohn, A. D., De Ferrari, G. V., and Kaykas, A. (2004) *Nat. Rev. Genet.* **5,** 691–701
69. Toledo, E. M., Colombres, M., and Inestrosa, N. C. (2008) *Prog. Neurobiol.* **86,** 281–296
70. Chenn, A., and Walsh, C. A. (2003) *Cereb. Cortex* **13,** 599–606
71. Chenn, A., and Walsh, C. A. (2002) *Science* **297,** 365–369
72. Viti, J., Gulacsi, A., and Lillien, L. (2003) *J. Neurosci.* **23,** 5919–5927
73. Israsena, N., Hu, M., Fu, W., Kan, L., and Kessler, J. A. (2004) *Dev. Biol.* **268,** 220–231